Nuclear Instruments and Methods in Physics Research B39 (1989) 130–135
North-Holland, Amsterdam

GRAIN GROWTH AND PHASE MORPHOLOGY IN ION BEAM MIXED, TWO PHASE Ni–Al AND Ni–Cr–Al ALLOYS

Dale ALEXANDER [1], Gary WAS [1] and James ERIDON [2]

[1] *University of Michigan, Department of Nuclear Engineering, Ann Arbor, Michigan 48109, USA*
[2] *Naval Research Laboratory, Surface Modifications Branch, Washington, DC 20375, USA*

Multilayers of Ni–21Al and Ni–20Cr–10Al were subjected to ion beam mixing using 350 keV Ni^+ ions and/or thermal annealing at 440 °C to study the development of grain growth and phase morphology. Two film thicknesses of Ni–21Al (60 and 120 nm) were investigated. Both thermal annealing and irradiation resulted in grain growth in the Ni–21Al samples. Grain size increased by a factor of 7 after irradiation and only 3–4 after annealing. Annealing produced a two phase $\gamma + \gamma'$ structure and nonuniform grain sizes while the irradiation produced a supersaturated solid solution with more uniform grain size. Annealing subsequent to irradiation produced a structure consisting of $\gamma + \gamma'$ and an HCP phase. There was no difference in grain growth behavior as a function of film thickness. The Ni–Cr–Al film exhibited no grain growth during annealing and only a factor of 6 increase during irradiation. Irradiation alone or post-irradiation annealing produced nearly identical structures of γ and the HCP phase. The γ' phase was never observed in the Ni–Cr–Al film. All irradiated samples showed a more uniform grain size compared to that following annealing. Considerable texture was observed in all irradiated samples in which the gamma grains in the film were aligned with the Ni grains in the substrate.

1. Introduction

Previous work [1] has shown that ion beam mixing of Ni–Al results in significant grain growth along with the formation of a unique dual phase gamma–gamma prime structure. This structure was shown to be stable against decomposition and grain growth during elevated temperature anneals for extended periods. However, little is known about the effects of ion energy, ion dose or annealing temperature on the formation and stability of the dual phase structure.

The present work addresses the effect of initial film thickness on ion induced grain growth and formation of the dual phase structure with composition Ni–21Al. This work also examines the effects of Cr on the formation of the dual phase structure. The Ni–Cr–Al system forms the basis of many of the high temperature, high strength superalloys, and thus ion beam mixing in this system may produce unique nonequilibrium microstructures with enhanced high temperature stability.

2. Experimental

Samples were prepared using 3 mm diameter disks punched from 0.25 mm thick, 99.998% pure nickel foil. The disks were annealed in an argon atmosphere at 1273 K for 4 h. The surfaces of the disks were successively polished with 600 grit SiC, alumina slurry, and Syton®. A short jet electropolish of the surface was provided as a final finish.

Evaporations were performed to provide three sets of samples with different compositions and thicknesses: 60 nm of Ni–21 at.% Al, 120 nm of Ni–21Al, and 60 nm of Ni–20Cr–10 Al. Multilayers were deposited on the Ni disks by electron beam evaporation in a vacuum system with base pressure $< 2 \times 10^{-7}$ Torr. The layer thicknesses were adjusted to provide the target surface compositions. The thickest layers did not exceed 6 nm. The evaporation rate typically varied between 0.1–0.5 nm/s. Rutherford backscattering analysis was performed on the 60 nm and 120 nm Ni–Al samples to verify the film composition.

Ion beam mixing of the layered structures was conducted in a Varian Extrion ion implanter at the Michigan Ion Beam Laboratory for Surface Modification and Analysis. Samples were irradiated at room temperature with 350 keV $^{58}Ni^+$ to a dose of 4×10^{16} ions/cm^2. The dose rate was typically 4.4×10^{12} ions/cm^2 s. This dose was chosen to achieve the same surface displacement damage (about 70 dpa as determined by TRIM [2]) produced in previous work with 500 keV Kr^+ ions [1]. The vacuum in the diffusion pumped end station during irradiation was nominally in the upper 10^{-7} Torr range. The temperature of the samples was monitored during irradiation by a thermocouple attached to the disk holder. The increase in the monitored temperature was no greater than 10 K.

0168-583X/89/$03.50

Both irradiated and unirradiated samples were annealed for 1 hour at 710 K in a cryopumped, stainless steel chamber. During the anneal the pressure in the system did not exceed 1×10^{-6} Torr. Following both irradiation and annealing, the disks were prepared for transmission electron microscopy (TEM). A protective lacquer was applied to the modified surface, and the disks were back-thinned in a jet electropolisher with a chilled solution (220 K) of 20% perchloric acid, 80% ethanol. The modified surface structures were studied using both bright and dark field imaging together with selected area diffraction (SAD) in a JEOL 2000FX scanning transmission electron microscope.

3. Results and discussion

Dark field imaging, using reflections from the (220) ring, was used to isolate grains and facilitate measurement of the average grain size for each of the treatments studied. Table 1 summarizes the average grain size of the three surface films investigated as a function of the surface treatment. Figs. 1 and 2 show the dark field images of grains resulting from the various treatments on the 120 nm Ni–Al and 60 nm Ni–Cr–Al samples, respectively. Because the (220) ring used for the dark field imaging is common to both the γ and γ' phases, the grains imaged in these figures could correspond to either phase. In the as-evaporated case, all three types of films exhibited a microstructure consisting of every fine, equiaxed grains, 8 nm in size.

The vacuum anneal at 710 K for 1 h produced grain growth to 35 nm and 21 nm in the 60 nm and 120 nm Ni–Al films, respectively. Fig. 1a shows a dark field image of the resulting grain structure in the 120 nm annealed sample in which nonuniform grain growth has occurred during annealing. No growth was observed in the annealed Ni–Cr–Al multilayers. The observance of grain growth in the annealed Ni–Al samples is in contrast to results of previous work in the Ni–Al system by Eridon et al. [1] who observed no grain growth after a similar annealing treatment. The only apparent difference between this work and Eridon's is that they used individual layer thicknesses approximately twice those used in this work. However, our results are not inconsistent with observations by Hentzell et al. [3] on the grain growth in Ni–Al films co-deposited onto substrates held at high temperature. Also, work by Liu et al. [4] on thin Ni films demonstrated nonuniform grain growth even after shorter, lower temperature anneals than were performed in this work.

Substantial ion beam induced grain growth was observed in all samples irradiated with 350 keV Ni^+ to a dose of 4×10^{16} ions/cm^2. Grain sizes averaged 61, 58, and 46 nm for the 60 nm Ni–Al, 120 nm Ni–Al, and 60 nm Ni–Cr–Al films, respectively. Unlike annealing, irradiation produced more uniform grain growth. The growth observed was of the same magnitude reported for Kr^+ irradiation of Ni–Al multilayer films [1] and irradiation of Ni films [4].

Post-irradiation annealing produced minimal additional grain growth. Thus the ultimate grain sizes achieved were 74, 64, and 52 nm for the 60 nm Ni–Al, 120 nm Ni–Al and 60 nm Ni–Cr–Al samples, respectively. The lack of a large difference in ultimate grain size in the 60 nm and 120 nm Ni–Al films is significant because it has been shown [5–7] that film thickness effects such as thermal grooving [8] can limit grain growth to a size which is a multiple of the film thickness. It is thus apparent that film thickness effects are not limiting grain growth in this case. The effect of dose on grain growth has not been specifically addressed, however, Liu et al. [4] demonstrated that saturation grain sizes are achieved in irradiated Ni films at doses approaching 1×10^{16} ions/cm^2. Since our dose was considerably higher than this, the observed grain sizes may well be at the saturated value.

Analysis of the phases present after surface treatment was conducted using selected area diffraction (SAD). Patterns for the 120 nm Ni–Al and 60 nm Ni–Cr–Al samples are shown in figs. 1 and 2 respectively, and a tabulation of all phases observed is included in table 1. Examination of the annealed 120 nm sample, fig. 1a, shows that in addition to the γ phase, superlattice rings belonging to the ordered γ' prime phase are present. These are the equilibrium phases predicted by the binary phase diagram for the composition Ni–21Al.

Table 1
Summary of average grain size (in nm) and observed phases for various surface treatments

	60 nm Ni–21 Al		120 nm Ni–21 Al		60 nm Ni–20Cr–10Al	
	Grain size	Phases	Grain size	Phases	Grain size	Phases
As-evaporated	8	γ	8	γ	8	γ, α
Annealed 1 h at 710 K	35	γ, γ'	21	γ, γ'	8	γ, α
Irradiated						
350 keV Ni^+ to 4×10^{16} ions/cm^2	61	γ, hcp?	58	γ, hcp?	46	γ, α, hcp
Irradiated + annealed	74	γ, γ', hcp	64	γ, γ', hcp	52	γ, α, hcp

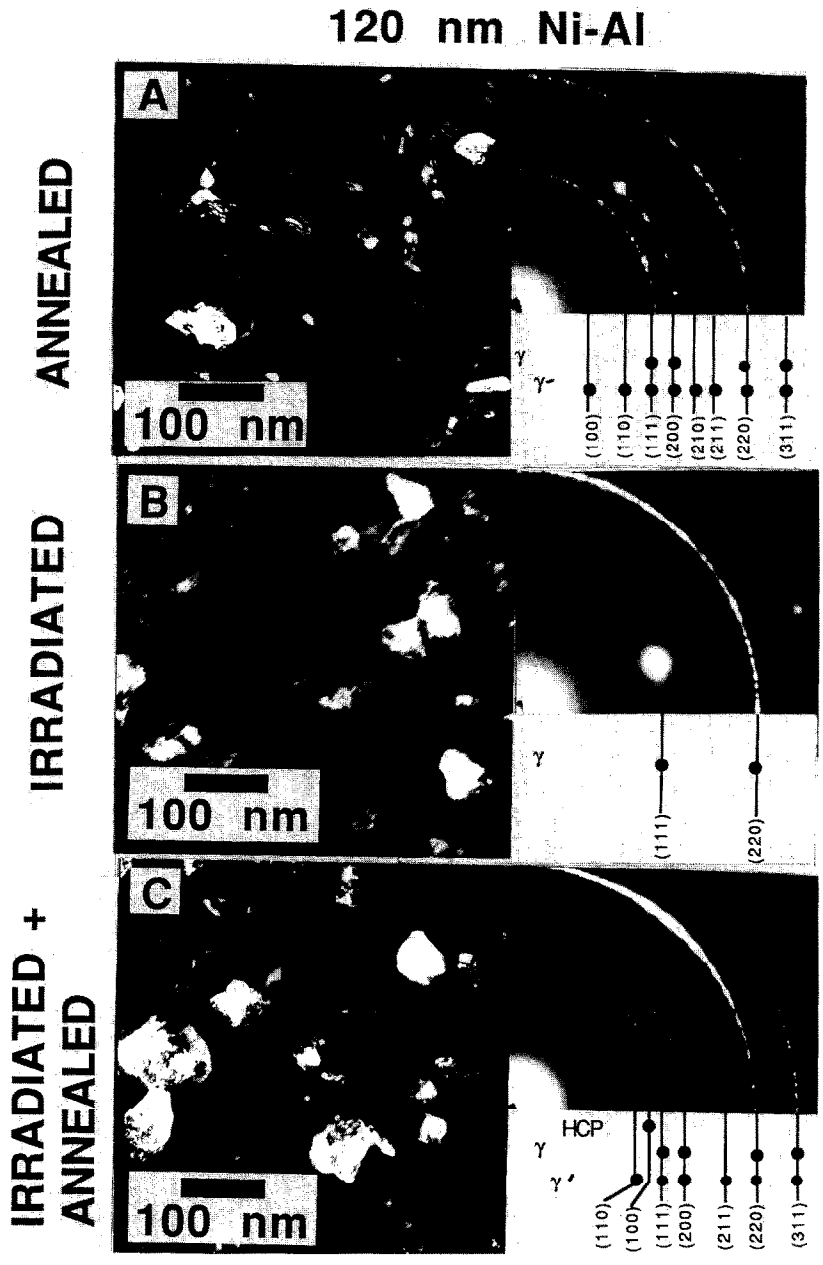

Fig. 1. Dark field images of microstructures and corresponding selected area electron diffraction patterns for treatments performed on 120 nm Ni–21Al: (A) annealed at 710 K for one hour, (B) irradiated with 350 keV Ni^+ to 4×10^{16} ions/cm^2, (C) irradiated with Ni^+ as in (B) then annealed as in (A). Dark field imaged using reflections from the 220 ring.

Irradiation of the 120 nm multilayers produced a nonequilibrium supersaturated solid solution of γ, fig. 1b. The SAD pattern shows a strong reflection from the (220) planes with a (111) ring partially discernible. No γ' rings are evident. The SAD pattern shown was photographed after tilting to display the entire (220) ring. Prior to tilting, considerable texture was observed in the (220) ring in the same direction as the (111) Ni substrate spots in the pattern. This texture indicates an alignment of the γ grains in the film with the substrate grains. Another possible explanation of the observed texture is found in the work of Van Wyk et al. [9] in which a strong (110) texture was seen in ion bombarded Cu films. They suggested that fcc crystallites oriented

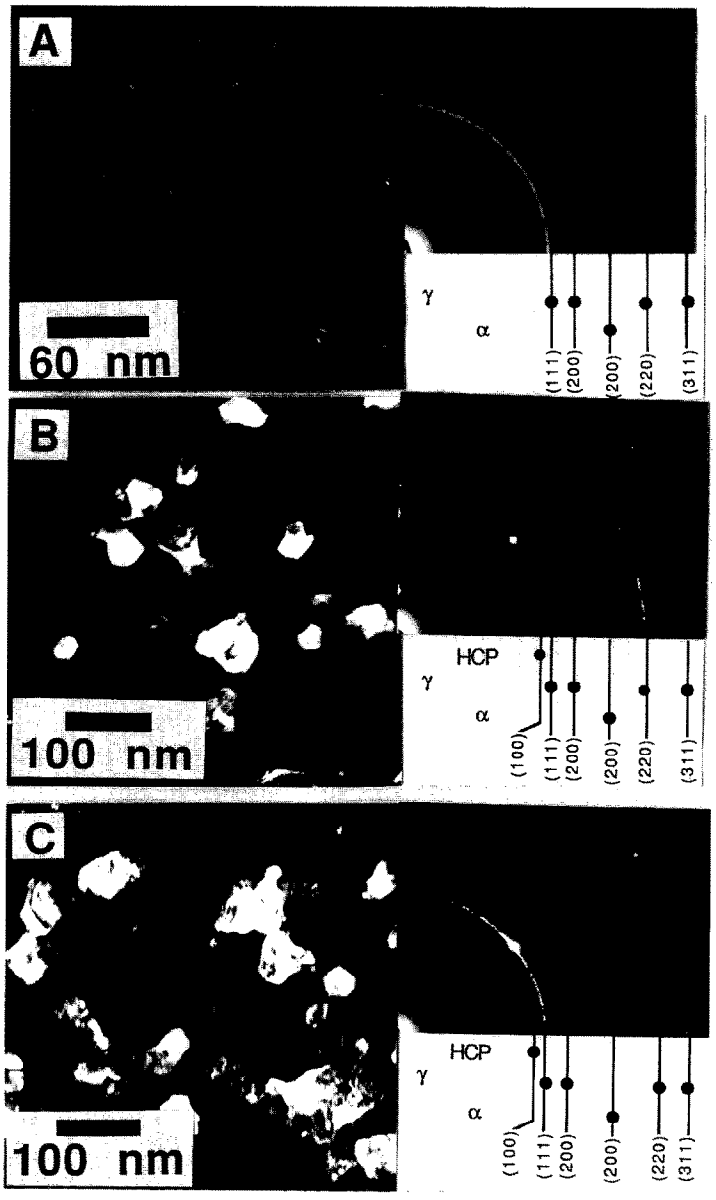

Fig. 2. Dark field images of microstructures and corresponding selected area electron diffraction patterns for treatments performed on 60 nm Ni–20Cr–10Al: (A) annealed at 710 K for one hour (note the change of scale), (B) irradiated with 350 kev Ni^+ to 4×10^{16} ions/cm^2, (C) irradiated with Ni^+ as in (B) then annealed as in (A). Dark field imaged using reflections from the (220) ring.

with the [110] direction parallel to the incident radiation suffer less damage (since the (110) plane has a lower atomic areal density compared to other crystallographic planes), and in turn the crystallites act as nucleation sites for other highly damaged grains.

Irradiation combined with post-irradiation annealing of the 120 nm samples produced the γ' phase as evidenced by the presence of both the (110) and the (211) γ' rings in the SAD pattern, fig. 1c. Texture is also apparent particularly in the (220) and (311) rings. Just inside the γ (111) ring is the (100) ring belonging to an HCP phase. This phase has been observed to occur in nickel rich Ni–Al after threshold irradiation at room temperature [10] and in Al^+ implantation into nickel [11]. The HCP phase is strongly textured with basal planes parallel to the plane of the film. This is evidenced by the absence of rings resulting from basal plane reflections in the SAD pattern in fig. 1c. Although

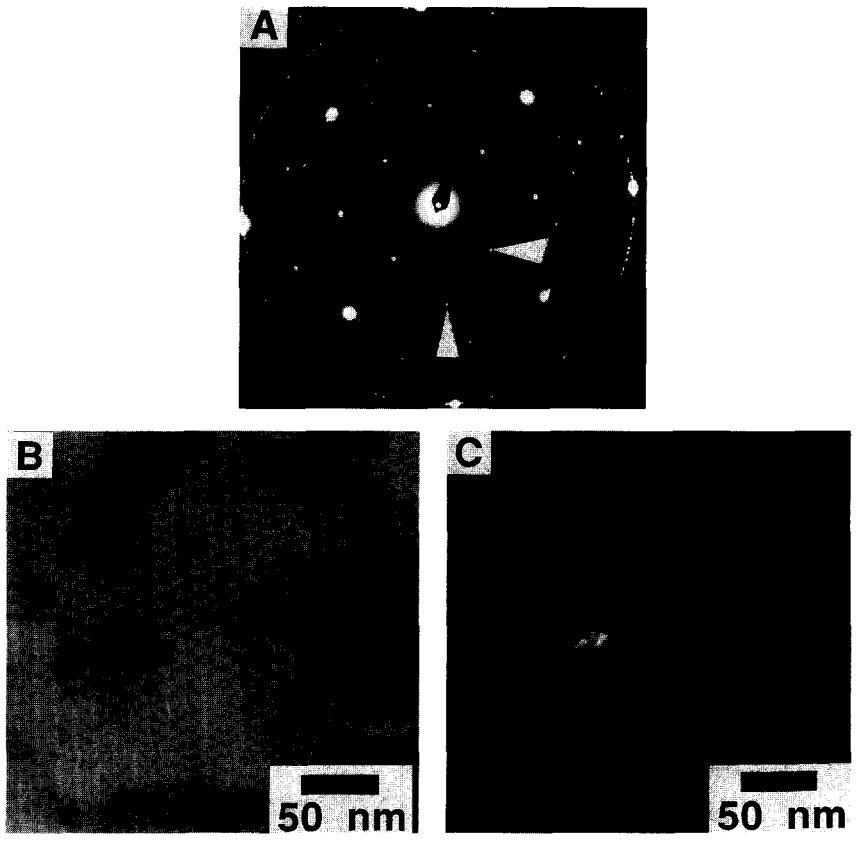

Fig. 3. (A) selected area diffraction pattern for annealed 60 nm Ni–21Al sample showing the presence of superlattice reflections as indicated by the arrows. (B) Bright field image of the are giving rise to diffraction in (A). (c) Dark field image of small γ' grains in (B) imaged using the (110) superlattice reflection identified by the bottom arrow in (A).

not evident in the diffraction patterns of fig. 1b, it is likely that the hcp phase was also present after irradiation of the multilayers as observed by others [10].

Annealing of the 60 nm Ni–Cr–Al samples at 710 K for one hour produced no change in the SAD pattern, fig. 2a, which appears to be identical to the as-evaporated case. The composition of this sample is such that it should lie in the two phase $\gamma + \gamma'$ region of the equilibrium ternary phase diagram [12]. Assuming homogenization and equilibrium were achieved as in the 120 nm Ni–Al samples, γ' lines should be evident, but clearly are not. Further, the Cr (α phase) (200) ring remains.

The SAD pattern for the irradiated Ni–Cr–Al samples shows rings corresponding to the γ phase and the HCP phase, fig. 2b, similar to irradiated Ni–Al, Fig. 1b. In addition the Cr (200) ring is still faintly present and has a slight texture corresponding to the texture of the γ (220) ring. The (111) ring also exhibits texture in the same direction as the Ni (111) substrate spots.

Annealing of the irradiated samples produced an SAD pattern, fig. 2c, which looks nearly identical to the as-irradiated case. Again, in addition to the γ phase, the presence of the HCP and Cr-α phases are also evident. The γ (111) ring displays texture in the direction of the (111) substrate spots.

It should be noted that composition of the Ni–Cr–Al samples were not verified quantitatively. Thus, uncertainty about composition precludes definitive statements about phase formation in these samples. However, the persistence of the Cr-α phase throughout all treatments is indeed puzzling and requires further study.

One final point warrants some discussion. A region of the film in the 60 nm Ni–21Al sample was observed in SAD to show reflections corresponding to superlattice spots in addition to superlattice rings, fig. 3a. Dark field imaging performed on a γ' (110) superlattice spot showed that the reflection was coming from grains approximately 20 nm in size, fig. 3c. Although more extensive dark field imaging of the γ' is needed, this observation suggests that the γ' in the film is of a smaller grain size than the γ grains and thus might explain the nonuniform grain size observed for annealed Ni–Al samples. The spotty appearance of γ rings versus the fine structure of the γ' rings in these annealed samples further supports this suggestion.

4. Conclusions

Substantial ion induced grain growth was observed in all samples irradiated with 350 keV Ni^+ ions to a dose of 4×10^{16} ions/cm^2. Grain sizes increased typically by a factor of 7 over the as-evaporated grain size. Thermal annealing of multilayers at 710 K for one hour produced only a 3–4 fold increase in grain size for the Ni–Al samples, and no observable growth in the Ni–Cr–Al samples. Further, considerable nonuniformity was observed in grain sizes for the annealed samples in contrast to the uniform sizes of the irradiated ones. Post-irradiation annealing resulted in minimal grain growth in all samples. The ultimate grain sizes achieved in the 60 nm thick films compared with the 120 nm films were nearly the same. This indicated that film thickness effects were not limiting the achievable grain size to a dose of 4×10^{16} ions/cm^2. Further work is underway to examine dose variations on grain size for both the Ni–Al and Ni–Cr–Al systems.

Annealing of multilayers resulted in the formation of γ and γ' equilibrium phases. Ion irradiation resulted in a supersaturated solid solution of γ phase and probably the HCP phase. Considerable texture arose in all the irradiated samples in which the film grains tended to align with the substrate grains. Post-irradiation annealing caused γ' to form but failed to remove the HCP phase.

Analysis of the phases in the Ni–Cr–Al samples indicated that gamma prime failed to form in all treatments even though the composition was clearly within the 2 phase $\gamma + \gamma'$ region of the ternary phase diagram. The HCP phase was formed following irradiation or irradiation + annealing treatments. The Cr-α phase was present after all treatments.

The authors gratefully acknowledge the staff and the use of the facilities at the Michigan Ion Beam Laboratory for Surface Modification and Analysis at the University of Michigan, as well as the support of D. Alexander by the DOE Nuclear Engineering, Health Physics and Radioactive Waste Management Fellowship Program. This work was funded by the national Science Foundation under grant #DMR8603174.

References

[1] J.M. Eridon, G.S. Was and L. Rehn, J. Appl. Phys. 62 (1987) 2145.
[2] J.P. Biersack and L.G. Haggmark, Nucl. Instr. and Meth. 174 (1980) 257.
[3] H.T.G. Hentzell, B. Andersson and S.E. Karlsson, Acta Metall. 31 (1983) 2103.
[4] J.C. Liu and J.W. Mayer, Nucl. Instr. and Meth. B19/20 (1987) 538.
[5] P. Wissman, Thin Solid Films 6 (1970) R67.
[6] A. Gangulee, S. Krongelb and G. Das, Thin Solid Films 24 (1974) 273.
[7] A. Gangulee, J. Appl. Phys. 45 (1974) 3749.
[8] W.W. Mullins, Acta Metall. 6 (1958) 414.
[9] G.N. Van Wyk and H.J. Smith, Nucl. Instr. and Meth. 170 (1980) 433.
[10] J.M. Eridon, G.S. Was and L. Rehn, J. Mater. Res. 3(4) (1988) 626.
[11] M. Ahmed and D.I. Potter, Acta Metall. 33 (1985) 2221.
[12] A. Taylor and R.W. Floyd, J. Institute of Metals 81 (1952) 451.